Computational Investigation of the Oxidative Deboronation of Boroglycine, $H_2N-CH_2-B(OH)_2$, Using H_2O and H_2O_2

Joseph D. Larkin,[†] George D. Markham,[§] Matt Milkevitch,[‡] Bernard R. Brooks,[†] and Charles W. Bock*[,‡,§]

The National Institutes of Health, National Heart, Lung, and Blood Institute, 5635 Fishers Lane, Rockville, Maryland 20852, Department of Chemistry and Biochemistry, School of Science and Health, Philadelphia University, School House Lane and Henry Avenue, Philadelphia, Pennsylvania 19144, and The Institute for Cancer Research, Fox Chase Cancer Center, 333 Cottman Avenue, Philadelphia, Pennsylvania 19111

Received: May 4, 2009; Revised Manuscript Received: August 10, 2009

We report results from a computational investigation of the oxidative deboronation of boroglycine, $H_2N-CH_2-B(OH)_2$, using H_2O and H_2O_2 as the reactive oxygen species (ROS) to yield aminomethanol, H_2N-CH_2-OH; these results complement our study on the protodeboronation of boroglycine to produce methylamine, H_2N-CH_3 (Larkin et al. *J. Phys. Chem. A* **2007**, *111*, 6489−6500). Second-order Møller−Plesset (MP2) perturbation theory with Dunning−Woon correlation-consistent (cc) basis sets were used for the calculations with comparisons made to results from density functional theory (DFT) at the PBE1PBE/6-311++G(d,p)(cc-pVDZ) levels. The effects of a bulk aqueous environment were also incorporated into the calculations employing PCM and CPCM methodology. Using H_2O as the ROS, the reaction H_2O + $H_2N-CH_2-B(OH)_2 \rightarrow H_2N-CH_2-OH + H-B(OH)_2$ was calculated to be endothermic; the value of ΔH^0_{298} was +12.0 kcal/mol at the MP2(FC)/cc-pVTZ computational level in vacuo and +13.7 kcal/mol in PCM aqueous media; the corresponding value for the activation barrier, $\Delta H^{\ddagger}$, was +94.3 kcal/mol relative to the separated reactants in vacuo and +89.9 kcal/mol in PCM aqueous media. In contrast, the reaction H_2O_2 + $H_2N-CH_2-B(OH)_2 \rightarrow H_2N-CH_2-OH + B(OH)_3$ was calculated to be highly exothermic with an ΔH^0_{298} value of −100.9 kcal/mol at the MP2(FC)/cc-pVTZ computational level in vacuo and −99.6 kcal/mol in CPCM aqueous media; the highest-energy transition state for the multistep process associated with this reaction involved the rearrangement of $H_2N-CH_2-B(OH)(OOH)$ to $H_2N-CH_2-O-B(OH)_2$ with a $\Delta H^{\ddagger}$ value of +23.2 kcal/mol in vacuo relative to the separated reactants. These computational results for boroglycine are in accord with the experimental observations for the deboronation of the FDA approved anticancer drug bortezomib (Velcade, PS-341), where it was found to be the principle deactivation pathway (Labutti et al. *Chem. Res. Toxicol.* **2006**, *19*, 539−546).

Introduction

Although boronic acids ($R-B(OH)_2$) have not been found in nature, they have emerged as an important class of compounds with diverse applications in a variety of fields.[1−5] In chemistry and material science, applications include sensors for 1,2- and 1,3-diols,[6−14] affinity ligands in chromatographic protocols,[15−20] and as submicrometer-scale devices.[21−24] In synthetic organic chemistry, the properties of boronic acids as mild Lewis acids have made them an attractive class of intermediates[25] that have been widely used in Suzuki cross-coupling reactions,[3,26] Diels−Alder reactions,[27] asymmetric synthesis of amino acids,[28] selective reduction of aldehydes,[29] and carboxylic acid activation.[30,31] Biochemical and medicinal applications of boronic acids include inhibitors of serine proteases and β-lactamases,[32−34] bioconjugates,[35] transmembrane transporters,[36−39] anti-HIV drugs,[40,41] substrates for protein immobilization,[42] and agents in neutron capture therapy.[43−45]

A particularly interesting and relevant example of the use of boronic acids in medicine involves the drug bortezomib (Velcade, PS-341),[46,47] which is a dipeptide boronic acid analogue that is currently FDA approved for the treatment of refractory multiple myeloma, a bone marrow cancer that affects 2 to 3 people per 100 000.[46,47] Bortezomib, a boronic acid analog of a Phe−Leu dipeptide coupled to a 2-carboxylpyrazine group (Figure 1) is a selective and highly effective inhibitor of the 26S proteasome, a large multicatalyic protease complex whose function is to regulate a variety of cellular functions by protein ubiquitation and degradation.[48,49] It is suspected that bortezomib produces cell death by causing an accumulation of misfolded/damaged proteins, inducing endoplasmic reticulum (ER) stress by overwhelming cellular mechanisms of coping with this buildup (the unfolded protein response, UPR) and triggering a unique pathway of apoptosis.[50] Because of the ability of bortezomib to induce ER stress, it is currently being investigated as a sensitizing agent in therapeutic regimens, for example, for pancreatic cancer, where it apparently induces cell death by an ER stress-dependent mechanism.[50] To a large extent, the potency of bortezomib is a result of the presence of the boronic acid moiety, which appears to form a tetrahedral intermediate analog with the active site N-terminal threonine residue of the proteasome.[51] Oxidative deboronation has been suggested as a principle route for the metabolism of bortezomib[52,53] representing

* Corresponding author. Tel: (215) 951-1976. E-mail: bockc@philau.com.
[†] National Heart, Lung, and Blood Institute.
[‡] Philadelphia University.
[§] The Institute for Cancer Research.

10.1021/jp904149w CCC: $40.75
Published on Web 09/18/2009

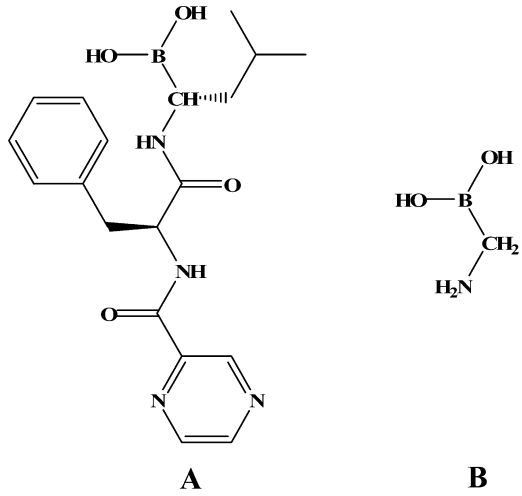

Figure 1. Structures of (A) bortezomib and (B) boroglycine.

a deactivation pathway for this chemotherapeutic agent,[53] yet no chemical mechanism has been elucidated for this process.

In the present article, we report our results from the first computational study of possible oxidative deboronation mechanisms for boroglycine, $H_2N-CH_2-B(OH)_2$, using H_2O and H_2O_2 as the reactive oxygen species (ROS). Boroglycine, a boronic acid analog of the amino acid glycine, serves as a simple model for the boronic component of the anticancer drug bortezomib. (See Figure 1.) Furthermore, several derivatives of boroglycine, including some isoelectronic and isostructural analogs, have shown promise as chymotrypsin inhibitors,[54,55] and more recently the peptide L-γ-Gly-L-Leu-aminomethyl boronic acid has been shown to be a stronger inhibitor of glutathionyl spermidine synthetase than the phosphonic acid analog, making it an attractive target for the design of antiparasitic drugs[56] and prompting interest in the properties of boroglycine in itself.

Computational Methods

Equilibrium geometries of the molecules involved in this article were obtained using second-order Møller−Plesset perturbation theory (MP2);[57] the frozen core (FC) option, which neglects core−electron correlation, was employed in all cases. Dunning−Woon cc-pVDZ, aug-cc-pVDZ, cc-pVTZ, and aug-cc-pVTZ basis sets[58−61] were used in the calculations. Frequency analyses were performed analytically to determine whether the optimized structures were local minima or transition states on the PES and to correct reaction energies to 298 K. Intrinsic reaction coordinate (IRC) analyses were employed in all cases to identify unambiguously the reactants and products associated with all of the transition states we located.[62,63] The calculations were performed using the Gaussian 03 suite of programs.[64] Atomic charges were obtained from natural population analyses (NPA), and the bonding was analyzed with the aid of natural bond orbitals (NBOs).[65−68]

Calculations using MP2 methodology with correlation-consistent basis sets are not currently practical for investigations of larger boron derivatives of significant chemical interest. Density functional theory (DFT), utilizing Pople-style basis sets,[69,70] provide an economical alternative to MP2, but the reliability of specific functional/basis-set combinations for describing the incredibly diverse range of boron chemistry[71] has yet to be fully established.[37−40] Therefore, we have compared our MP2/(cc-pVDZ, aug-cc-pVDZ, and cc-pVTZ) results with those from more computationally efficient DFT methodologies using the PBE1PBE/6-311++G(d,p)(cc-pVDZ) levels;[72] the PBE1PBE functional, in combination with either Pople-style or correlation-consistent basis sets, has shown promise in describing a variety of aspects of boron chemistry.[73−78] It should be noted that it is well established that the hybrid B3LYP functional has significant problems in dealing with some aspects of boron chemistry, most notably dative bonding.[73−80]

Results from continuum solvation models were employed to assess the effects of a bulk aqueous environment on the gas-phase results. We used the following implicit solvation models: (1) the IEF polarizable continuum model (PCM) model, developed by Tomasi and coworkers[81−86] at the PBE1PBE/6-311++G(d,p) and MP2/6-311++G(d,p)(cc-pVTZ) computational levels, and (2) the conductorlike PCM model (CPCM), introduced by Barone and Cossi[87,88] at the MP2/6-311++G(d,p)(cc-pVTZ) computational levels. (The UAKS cavity was used for the CPCM solvent model on the basis of the performance indicated by Takano and Houk.[89]) Such implicit solvation models, however, provide only a description of long-range solute−solvent interactions and, as a consequence, have significant limitations in describing protic solvents.[90,91] Therefore, in some cases, explicit water molecules were used to provide a description of the short-range, site-specific effects of an aqueous environment on the hydrogen-bonding or the boron dative-bonding interactions relevant to the oxidative deboronation mechanisms of boroglycine that we explored.

Results and Discussion

In this section, we present calculated thermodynamic/kinetic data relevant to the oxidative deboronation of $H_2N-CH_2-B(OH)_2$ with H_2O and HOOH. To a large extent, the oxidative reactivity of the C−B bond is a consequence of the huge difference between the B−O and B−C bond energies.[1,92]

To our knowledge, no experimental data are currently available regarding the structure of boroglycine; however, results from a computational investigation of the geometrical structures and relative energies of various conformers of $H_2N-CH_2-B(OH)_2$ as well as its constitutional isomer $H_3C-NH-B(OH)_2$ have been reported by Larkin et al.[76] in their investigation of possible protodeboronation mechanisms of $H_2N-CH_2-B(OH)_2$; these results provided a basis for the present study.

Oxidative Cleavage using H_2O. We initially considered H_2O as a possible oxidative agent to establish a thermochemical baseline for the conversion of boroglycine to aminomethanol. Thermodynamic parameters for the reaction

$$H_2O + H_2N-CH_2-B(OH)_2 \rightarrow H_2N-CH_2-OH + HB(OH)_2 \quad (1)$$

are listed in Table 1. This reaction was calculated to be endothermic in vacuo; the values of ΔH^0_{298} are +11.3, +12.0, and +13.3 kcal/mol at the PBE1PBE/6-311++G(d,p), MP2/cc-pVTZ, and MP2/aug-cc-pVTZ levels, respectively. In aqueous media, the values of ΔH^0_{298} for various implicit solvation models were +13.4 kcal/mol at the PCM(PBE1PBE/6-311++G(d,p)) level, +13.7 kcal/mol at the PCM(MP2/cc-pVTZ) level, +10.6 kcal/mol at the CPCM(PBE1PBE/6-311++G(d,p)) level, and +11.1 at the CPCM(MP2/cc-pVTZ) level. (See Table 1S of the Supporting Information.) Although the corresponding PCM and CPCM values of ΔH^0_{298} lie on opposite sides of the gas-phase values, neither of these implicit solvation models imply a major role for the long-range effects of an aqueous environment. For comparison, we note that the

TABLE 1: Thermodynamic Parameters (kilocalories per mole) for the Reactions of $H_2N-CH_2-B(OH)_2$ with (A) H_2O and (B) H_2O_2

	(A) H_2O			
	PBE1PBE/	MP2(FC)/		
	6-311++G(d,p)	cc-pVDZ	aug-cc-pVDZ	cc-pVTZ
$H_2N-CH_2-B(OH)_2 + H_2O \rightarrow H_2N-CH_2-OH + HB(OH)_2$				
ΔE	+11.0	+9.8	+14.1	+11.6
ΔH^0_{298}	+11.3	+10.2	+14.4	+12.0
ΔG^0_{298}	+11.1	+9.7	+14.1	+11.7
	(B) H_2O_2			
	PBE1PBE/	MP2(FC)/		
	6-311++G(d,p)	cc-pVDZ	aug-cc-pVDZ	cc-pVTZ
$H_2N-CH_2-B(OH)_2 + H_2O_2 \rightarrow H_2N-CH_2-OH + B(OH)_3$				
ΔE	−98.9	−100.2	−100.3	−102.4
ΔH^0_{298}	−97.7	−98.6	−98.9	−100.9
ΔG^0_{298}	−96.4	−97.6	−97.6	−100.1
$H_2N-CH_2-B(OH)_2 + H_2O_2 \rightarrow H_2N-CH_2-B(OH)(OOH) + H_2O$				
ΔE	−1.4	−0.1	−2.3	−0.9
ΔH^0_{298}	−2.0	−0.7	−2.9	−1.5
ΔG^0_{298}	−1.6	−0.1	−2.0	−1.4
$H_2N-CH_2-B(OH)(OOH) \rightarrow H_2N-CH_2-O-B(OH)_2$				
ΔE	−97.7	−100.6	−100.9	−103.0
ΔH^0_{298}	−96.3	−98.9	−99.2	−101.4
ΔG^0_{298}	−94.6	−97.9	−97.6	−99.4

TABLE 2: Kinetic Parameters (kilocalories per mole) for Reactions of $H_2N-CH_2-B(OH)_2$ with (A) H_2O and (B) H_2O_2

	(A) H_2O			
	PBE1PBE//	MP2(FC)//		
	6-311++G(d,p)	cc-pVDZ	aug-cc-pVDZ	cc-pVTZ
$H_2N-CH_2-B(OH)_2 + H_2O \rightarrow TS \rightarrow H_2N-CH_2-OH + HB(OH)_2$				
$\Delta E^{\ddagger}$	+87.3	+97.1	+92.0	+95.5
$\Delta H^{\ddagger}$	+85.6	+95.9	+90.6	+94.3
$\Delta G^{\ddagger}$	+95.3	+104.9	+100.0	+103.6
	(B) H_2O_2			
	PBE1PBE//	MP2(FC)//		
	6-311++G(d,p)	cc-pVDZ	aug-cc-pVDZ	cc-pVTZ
$H_2N-CH_2-B(OH)_2 + H_2O_2 \rightarrow TS \rightarrow H_2N-CH_2-B(OH)(OOH) + H_2O$				
$\Delta E^{\ddagger}$	+20.0	+15.3	+16.8	+16.9
$\Delta H^{\ddagger}$	+18.0	+13.5	+14.8	+15.1
$\Delta G^{\ddagger}$	+30.4	+26.5	+27.7	+27.8
$H_2N-CH_2-B(OH)(OOH) + H_2O \rightarrow TS \rightarrow H_2N-CH_2-O-B(OH)_2 + H_2O$				
$\Delta E^{\ddagger}$	+18.9	+20.8	+24.3	+23.7
$\Delta H^{\ddagger}$	+18.2	+20.4	+23.8	+23.2
$\Delta G^{\ddagger}$	+31.2	+33.6	+36.7	+36.5

protodeboronation reaction of boroglycine, that is, $H_2O + H_2N-CH_2-B(OH)_2 \rightarrow B(OH)_3 + H_2N-CH_3$, was calculated to be substantially exothermic at similar levels in vacuo, with values of ΔH^0_{298} in the −20 to −30 kcal/mol range.[76,93]

Several conformations of transition states (TSs) were obtained for reaction 1, one of which is shown in Figure 2. The calculated activation barrier for this TS was extremely high; the values of $\Delta H^{\ddagger}$ were +85.6 and +94.3 at the PBE1PBE/6-311++G(d,p) and MP2/cc-pVTZ levels, respectively, relative to the separated reactants in vacuo. (See Table 2.) In aqueous media, the values of the activation barrier for reaction 1 using several implicit solvation models were +84.2, +88.7, +88.2, and +89.8 at the PCM(PBE1PBE/6-311++G(d,p)), PCM(MP2/6-311++G(d,p)), CPCM(PBE1PBE/6-311++G(d,p)), and CPCM(MP2/6-311++G(d,p)) levels, respectively. (See Table 2S of the Supporting Information.) The structure of this TS for reaction 1 clearly identifies the water−oxygen atom as a nucleophile attacking the α-carbon atom of boroglycine; the extremely high calculated activation barrier for this reaction is in accord with the nearly complete heterolytic breaking of the carbon−boron bond and the concomitant formation of a boranion and a methaniminium ion (Figure 2); the MP2/cc-pVTZ NPA charge on the boron atom in this TS was +0.39e, compared with +1.02e and +0.91e in the reactant and product, respectively, showing a considerable transfer of electron density to the boron atom from the H_2N-CH_2 moiety at the TS. These findings provide computational support for the observation that oxidative cleavage of the B−C bond of boronic acid derivatives in air is a kinetically slow process.[1] The corresponding activation barriers for the protodeboronation reaction

$$H_2O + H_2N-CH_2-B(OH)_2 \rightarrow B(OH)_3 + H_2N-CH_3 \quad (2)$$

in which the water−oxygen atom attacks the boron atom were found to be much lower, +36.1 and +34.6 kcal/mol in vacuo at the PBE1PBE/6-311++G(d,p) and MP2/cc-pVTZ levels, respectively.[76]

It should be noted that boroglycine is also susceptible to a 1,2-carbon-to-nitrogen migration of the $-B(OH)_2$ moiety.[1,94−98] Indeed, this conversion of $H_2N-CH_2-B(OH)_2$ to $H_3C-NH-B(OH)_2$ is thermodynamically favored; for example, the calculated values of ΔH^0_{298} were −18.0 and −19.4 kcal/mol in vacuo at the PBE1PBE/6-311++G(d,p) and MP2/cc-pVTZ levels, and the corresponding values of ΔH^0_{298} in PCM aqueous media were similar.[76] The transition state for this 1,2-migration in vacuo and in PCM aqueous media was calculated to involve two very compact three-centered rings, and the activation barriers were computed to be extremely high: the values of $\Delta H^{\ddagger}$ were ∼+70 kcal/mol.[76] In the presence of one explicit water molecule, however, the barrier was dramatically lower; for example, the values of $\Delta H^{\ddagger}$ were only +27.0 and +28.8 kcal/mol at the PBE1PBE/6-311++G(d,p) and MP2/6-311++G(d,p) levels,

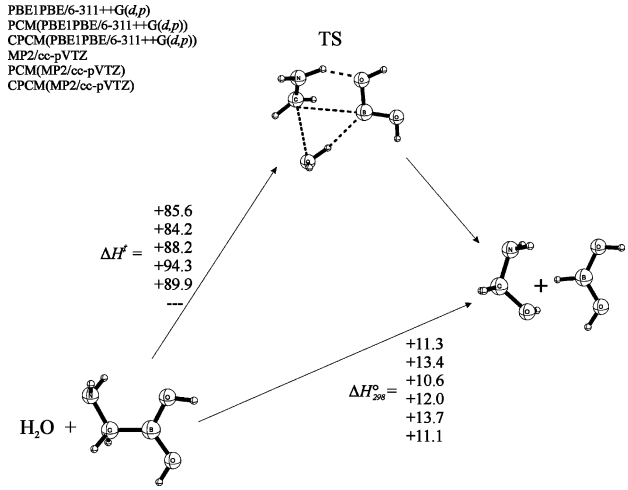

Figure 2. Mechanism for the reaction: $H_2O + H_2N-CH_2-B(OH)_2 \rightarrow H_2N-CH_2-OH + HB(OH)_2$.

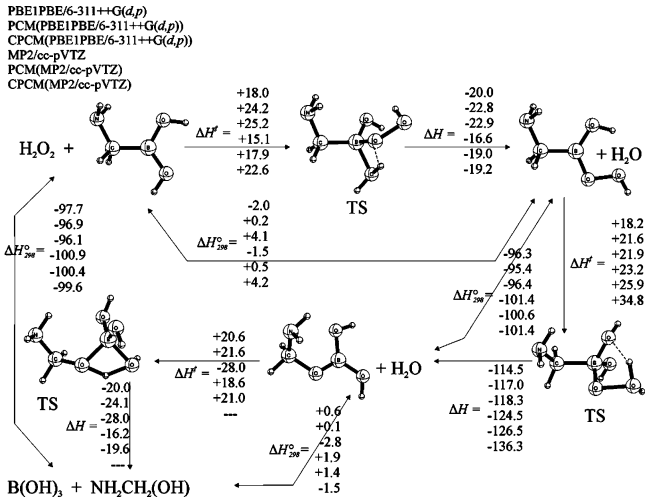

Figure 3. Mechanism for the Reaction: $H_2O_2 + H_2N-CH_2-B(OH)_2 \rightarrow H_2N-CH_2-OH + B(OH)_3$.

respectively,[76] emphasizing the importance of the short-range effects of surrounding water molecules on this shift mechanism.

In vacuo, as well as in the reaction field of water, the above thermochemical results clearly demonstrate that oxidative deboronation of boroglycine with a water molecule as the ROS is not competitive with the corresponding protodeboronation or with a 1,2-carbon-to-nitrogen (Matteson) rearrangement of the $-B(OH)_2$ group. In light of these results, we investigated the oxidative deboronation of boroglycine using hydrogen peroxide as the ROS.

Oxidative Cleavage using H_2O_2. As would be expected, calculated thermodynamic parameters for the oxidative deboronation of $H_2N-CH_2-B(OH)_2$ using H_2O_2 as the ROS, that is

$$H_2O_2 + H_2N-CH_2-B(OH)_2 \rightarrow H_2N-CH_2-OH + B(OH)_3 \quad (3)$$

show that this reaction is highly exothermic in vacuo; for example, the values of ΔH^0_{298} were -97.7 and -100.9 kcal/mol at the PBE1PBE/6-311++G(d,p) and MP2/cc-pVTZ levels (Table 1 and Figure 3); the corresponding values of ΔH^0_{298} in aqueous media were -96.9, -100.4, -96.1, and -99.6 kcal/mol at the PCM(PBE1PBE/6-311++G(d,p)), PCM(MP2/cc-pVTZ), CPCM(PBE1PBE/6-311++G(d,p)), and CPCM(MP2/cc-pVTZ) levels, respectively (Table 1S in the Supporting Information; values of ΔH^0_{298} at other computational levels are also given in this table), quite similar to the corresponding values in vacuo, suggesting a relatively small effect of long-range dielectric interactions with water on the thermodynamics of this reaction.

For comparison, we note that the corresponding protodeboronation reaction

$$H_2O_2 + H_2N-CH_2-B(OH)_2 \rightarrow H_2N-CH_3 + B(OH)_2(OOH) \quad (4)$$

was also calculated to be significantly exothermic, but the values of ΔH^0_{298} for the same conformer of $H_2N-CH_2-B(OH)_2$ were considerably less negative: -27.4 and -29.4 kcal/mol in vacuo at the PBE1PBE/6-311++G(d,p) and MP2/cc-pVTZ levels and -24.5, -26.9, -19.9, and -22.7 kcal/mol in PCM(PBE1PBE/6-311++G(d,p)), PCM(MP2(FC)/cc-pVTZ), CPCM(PBE1PBE/6-311++G(d,p)), and CPCM(MP2(FC)/cc-pVTZ) levels in aqueous media. Remarkably, these enthalpy changes for the protodeboronation of boroglycine using H_2O_2 are only a few kilocalories per mole more negative than the corresponding changes using H_2O as the ROS.[76]

Despite an extensive search, no single-step mechanism for reaction 3 could be found in vacuo or in aqueous media,[99] and thus our attention turned to possible multistep mechanisms. (See Figure 3.) It appears that the initial step in this reaction involves the conversion of boroglycine to aminomethyl peroxy borinic acid,[100,101] that is

$$H_2N-CH_2-B(OH)_2 + H_2O_2 \rightarrow H_2N-CH_2-B(OH)(OOH) + H_2O \quad (5)$$

which was calculated to be just slightly exothermic; for example, the values of ΔH^0_{298} in vacuo were -2.0 and -1.5 kcal/mol at the PBE1PBE/6-311++G(d,p) and MP2/cc-pVTZ levels (Table 1; results at other levels are also listed in this table); the values of ΔH^0_{298} in implicit solvent were $+0.2$, $+0.5$, $+4.1$, and $+4.2$ kcal/mol at the PCM(PBE1PBE/6-311++G(d,p)), PCM(MP2/cc-pVTZ), CPCM(PBE1PBE/6-311++G(d,p)), and CPCM(MP2/cc-pVTZ) levels, respectively. The calculated values of the activation enthalpy for reaction 5 were $+18.0$ and $+15.1$ kcal/mol in vacuo at the PBE1PBE/6-311++G(d,p) and MP2/cc-pVTZ levels, respectively, relative to the separated reactants. (See Table 2 and Figure 3.) Using implicit solvation models, the activation enthalpies for reaction 5 were somewhat higher relative to the isolated reactants compared with the gas-phase results: PCM: PBE1PBE/6-311++G(d,p) = +24.2 kcal/mol and MP2/cc-pVTZ = +17.9 kcal/mol; CPCM: PBE1PBE/6-311++G(d,p) = +25.2 and MP2/cc-pVTZ = +22.6 kcal/mol.

The second step in the mechanism for reaction 3 above involves the rearrangement of $H_2N-CH_2-B(OH)(OOH)$ to $H_2N-CH_2-O-B(OH)_2$. (See Figure 3.) This isomerization is highly exothermic; for example, the computed values of ΔH^0_{298} were -96.3 and -101.4 kcal/mol in vacuo at the PBE1PBE/6-311++G(d,p) and MP2/cc-pVTZ levels; the corresponding values in aqueous media were: PCM: PBE1PBE/6-311++G(d,p) = -95.4 and MP2/cc-pVTZ = -100.6 kcal/mol; CPCM: PBE1PBE/6-311++G(d,p) = -96.4 kcal/mol and MP2/cc-pVTZ = -101.4 kcal/mol, respectively. In the presence of an explicit water molecule oriented initially to play an active role in the process (Figure 3), the values of $\Delta H^{\ddagger}$ for this rearrangement were calculated to be $+18.2$ and $+23.2$ kcal/mol in vacuo relative to $H_2N-CH_2-B(OH)(OOH)$ and H_2O at the PBE1PBE/6-311++G(d,p) and MP2/cc-pVTZ levels, respectively; the corresponding values relative to the isolated reactants, H_2O_2 and $H_2N-CH_2-B(OH)_2$, were $+16.2$ and $+21.7$ kcal/mol. In the reaction field of water, the values of $\Delta H^{\ddagger}$ were $+21.6$, $+25.9$, $+21.9$, and $+34.8$ kcal/mol using PCM(PBE1PBE/6-311++G(d,p)), PCM(MP2/cc-pVTZ), CPCM(PBE1PBE/6-311++G(d,p)), and CPCM(MP2/cc-pVTZ) methodology.

In the final step of this mechanism, $H_2N-CH_2-O-B(OH)_2$ is converted to $H_2N-CH_2(OH)$ and $B(OH)_3$. (See Figure 3.) This reaction, $H_2O + H_2N-CH_2-O-B(OH)_2 \rightarrow H_2N-CH_2(OH) + B(OH)_3$, is nearly thermoneutral where the values of ΔH^0_{298} are $+0.6$ and $+1.9$ kcal/mol in vacuo at the PBE1PBE/6-311++G(d,p) and MP2/cc-pVTZ levels, respectively; the value of ΔH^0_{298} in PCM (CPCM) implicit solvent at the PBE1PBE/6-311++G(d,p) and MP2/cc-pVTZ levels of theory are $+0.1$ ($+1.4$) and -2.8 (-1.5). The transition state for this process was also located, and the value of $\Delta H^{\ddagger}$ is $+20.6$ and

+18.6 kcal/mol in vacuo relative to isolated $H_2N-CH_2-O-B(OH)_2$ and H_2O at the PBE1PBE/6-311++G(d,p) and MP2/cc-pVTZ levels; the corresponding values in aqueous media were: PCM: PBE1PBE/6-311++G(d,p) = +21.6 kcal/mol and MP2/cc-pVTZ = +21.0 kcal/mol; CPCM: PBE1PBE/6-311++G(d,p) = +21.9 kcal/mol. (Our attempts to locate a transition state at the CPCM: MP2/cc-pVTZ level failed.)

Concluding Remarks

Boronic acids have emerged as an important class of compounds in chemistry, biochemistry, synthesis, medicine, and material science,[1−35,37−55,76,102] but much remains to be learned about their geometrical structures, thermodynamics, and kinetics in vacuo and in a variety of solvents as well as the reliability of various computational methods for describing the diverse range of boron chemistry.[71] In this article, we discussed our computational findings for the oxidative deboronation of boroglycine, $H_2N-CH_2-B(OH)_2$, using H_2O and H_2O_2 as the ROS in vacuo and in the reaction field of water.

Using H_2O as the ROS, the oxidative reaction, $H_2O + H_2N-CH_2-B(OH)_2 \rightarrow H_2N-CH_2-OH + H-B(OH)_2$, was calculated to be endothermic; the values of ΔH^0_{298} are +11.3, +12.0, and +13.3 kcal/mol at the PBE1PBE/6-311++G(d,p), MP2/cc-pVTZ, and MP2/aug-cc-pVTZ computational levels, respectively (Table 1); the corresponding values for the protodeboronation reaction: $H_2O + H_2N-CH_2-B(OH)_2 \rightarrow B(OH)_3 + H_2N-CH_3$, were found to be exothermic at similar levels, with values in the −20 to −30 kcal/mol range.[76] The values for the oxidative activation enthalpy, $\Delta H^{\ddagger}$, were predicted to be extremely high relative to the separated reactants, +85.6 and +94.3 kcal/mol, using PBE1PBE/6-311++G(d,p) and MP2/cc-pVTZ levels. Computed effects from implicit solvation models proved to be minimal on the thermodynamics of this oxidative mechanism.

Using H_2O_2 as the ROS, the oxidative reaction, $H_2O_2 + H_2N-CH_2-B(OH)_2 \rightarrow H_2N-CH_2-OH + B(OH)_3$, was calculated to be highly exothermic; the values of ΔH^0_{298} were −97.7 and −100.9 kcal/mol at the PBE1PBE/6-311++G(d,p) and MP2/cc-pVTZ levels, respectively; the corresponding protodeboronation reaction, $H_2O_2 + H_2N-CH_2-B(OH)_2 \rightarrow H_2N-CH_3 + B(OH)_2(OOH)$, was also calculated to be exothermic, but the values of ΔH^0_{298} were considerably less negative, −29.9 and −25.9 kcal/mol. This oxidative process proved to involve several steps (Figure 3); the highest-energy transition state for the multistep process involved the rearrangement of $H_2N-CH_2-B(OH)(OOH)$ to $H_2N-CH_2-O-B(OH)_2$, and the value of $\Delta H^{\ddagger}$ was +18.2 and +23.2 kcal/mol relative to the separated reactants at the PBE1PBE/6-311++G** and MP2/cc-pVTZ levels, respectively. These results provide computational support for the experimental results of Labutti et al.[53] that H_2O_2-mediated deboronation energetically favors an oxidative approach. Our results further suggest that this occurs via a multistep mechanism.

Acknowledgment. This research was partially supported (J.D.L. and B.R.B.) by the Intramural Research Program of the NIH, NHLBI. G.D.M. would like to thank the NIH (GM31186) and NCI (CA06927) for financial support of this work, which was also supported by an appropriation from the Commonwealth of Pennsylvania. The High Performance Computing Facility at the Fox Chase Cancer Center and the PQS Cluster Facility at Philadelphia University were used for the calculations described in this manuscript. This study also utilized the high-performance computational capabilities of the Biowulf Linux cluster at the National Institutes of Health, Bethesda, MD (http://biowulf.nih.gov).

Supporting Information Available: Thermodynamic parameters for the reactions of $H_2N-CH_2-B(OH)_2$ with H_2O and H_2O_2 using the PCM and CPCM implicit solvation models and kinetic parameters for the reactions of $H_2N-CH_2-B(OH)_2$ with H_2O and H_2O_2 using the PCM and CPCM implicit solvation models. This material is available free of charge via the Internet at http://pubs.acs.org.

References and Notes

(1) Hall, D. G. *Boronic Acids: Preparation and Applications in Organic Synthesis and Medicine*; Wiley-VCH Verlag: Weinheim, Germany, 2005.

(2) Yang, W.; Gao, X.; Wang, B. Boronic acid compounds as potential pharmaceutical agents. *Med. Res. Rev.* **2003**, *23*, 346–368.

(3) Miyaura, N.; Suzuki, A. Palladium-catalyzed cross-coupling reactions of organoboron compounds. *Chem. Rev.* **1995**, *95*, 2457–2483.

(4) Suzuki, A. *Metal-Catalyzed Cross-Coupling Reactions*; Wiley-VCH: Weinheim, Germany, 1998.

(5) Abu Ali, H.; Dembitsy, V. M.; Srebnic, M. *Contemporary Aspects of Boron Chemistry and Biological Applications*; Elsevier: Boston, 2005.

(6) Franzen, S.; Ni, W.; Wang, B. Study of the mechanism of electron-transfer quenching by boron−nitrogen adducts in fluorescent sensors. *J. Phys. Chem. B* **2003**, *107*, 12942–12948.

(7) Koumoto, K.; Takenchi, M.; Shinkai, S. Design of visualized sugar sensing system utilizing a boronic acid−azopyridine interaction. *Supramol. Chem.* **1998**, *9*, 203.

(8) Ni, W.; Fang, H.; Springsteen, G.; Wang, B. The design of boronic acid spectroscopic reporter compounds by taking advantage of the pK(a)-lowering effect of diol binding: nitrophenol-based color reporters for diols. *J. Org. Chem.* **2004**, *69*, 1999–2007.

(9) Otsuka, H.; Uchimura, E.; Koshino, H.; Okano, T.; Kataoka, K. Anomalous binding profile of phenylboronic acid with *N*-acetylneuraminic acid (Neu5Ac) in aqueous solution with varying pH. *J. Am. Chem. Soc.* **2003**, *125*, 3493–3502.

(10) Philips, M. D.; James, T. D. Boronic acid based modular fluorescent imaging of glucose. *J. Fluoresc.* **2004**, *14*, 549–559.

(11) Springsteen, G.; Wang, B. A detailed examination of boronic acid-diol complexation. *Tetrahedron* **2002**, *58*, 5291–5300.

(12) Steiegler, S. Selective carbohydrate recognition by synthetic receptors in aqueous solution. *Curr. Org. Chem.* **2003**, *7*, 81–102.

(13) Wang, W.; Gao, X.; Wang, B. Boronic-acid based sensors for carbohydrates. *Curr. Org. Chem.* **2002**, *6*, 1285–1317.

(14) James, T. D. Saccharide-selective boronic acid based photoinduced electron transfer (PET) fluorescent sensors. *Top. Curr. Chem.* **2007**, *277*, 107–152.

(15) Li, X.-C.; Scouten, W. H. New ligands for boronate affinity chromatography. *J. Chromatogr., A* **1994**, *687*, 61–69.

(16) Wulff, G. Molecular imprinting in cross-linked materials with the aid of molecular templates: a way towards artificial. *Angew. Chem., Int. Ed. Engl.* **1995**, *34*, 1812–1832.

(17) Westmark, P. R.; Valencia, L. S.; Smith, B. D. Influence of eluent anions in boronate affinity chromatography. *J. Chromatogr., A* **1994**, *664*, 123–128.

(18) Liu, G.; Hubbard, J. L.; Scouten, W. H. Synthesis and structural investigation of two potential boronate affinity chromatography ligands catechol [2-(diethylamino)carbonyl, 4-methyl]phenylborante. *J. Organomet. Chem.* **1995**, *493*, 91–94.

(19) Psotova, L. Boronate affinity-chromatography and the ap. *Chem. Listy* **1995**, *89*, 641–648.

(20) Prokopcová, H.; Kappe, C. O. Desulfitative carbon-carbon cross-coupling of thioamide fragments with boronic acids. *Adv. Synthesis Catalysis* **2007**, *349*, 448–452.

(21) Li, Y.; Ruoff, R. S.; Chang, R. P. H. Boric acid nanotubes, nanotips, nanorods, microtubes, and microtips. *Chem. Mater.* **2003**, *15*, 3276–3285.

(22) Wang, W.; Zhang, Y.; Huang, K. Prediction of a family of cage-shaped boric acid clusters. *J. Phys. Chem. B* **2005**, *109*, 8562–8564.

(23) Wang, W.; Zhang, Y.; Huang, K. Self-curl and self-assembly of boric acid clusters. *Chem. Phys. Lett.* **2005**, *405*, 425–428.

(24) Parry, P. R.; Wang, C.; Batsanov, A. S.; Bryce, M. R.; Tarbit, B. Functionalized pyridylboronic acids and their Suzuki cross-coupling reactions to yield novel heteroarylpyridines. *J. Org. Chem.* **2002**, *67*, 7541–7543.

(25) Ferrier, R. J. Carbohydrate boronates. *Adv. Carbohydr. Chem. Biochem.* **1978**, *35*, 31–80.

(26) John, J.; Sajisha, V. S.; Mohanlad, S.; Radhakrishnan, K. V. Iodine assisted modified Suzuki type reaction of bicyclic hydrazines: steroselective synthesis of functionalized cyclopentenes. *Chem. Commun.* **2006**, 33.

(27) Ishihara, K.; Yamamoto, H. Arylboron compounds as acid catalysts in organic synthetic transformations. *Eur. J. Org. Chem.* **1999**, 527–538.

(28) Yu, H.; Wang, B. Phenylboronic acids facilitated selective reduction of aldehydes by tributyltin hydride. *Synth. Commun.* **2001**, *31*, 163–169.

(29) Petasis, N. A.; Zavialov, I. A. A new and practical synthesis of alpha-amino acids from alkenyl boronic acids. *J. Am. Chem. Soc.* **1997**, *119*, 445–446.

(30) Latta, R.; Springsteen, G.; Wang, B. Development and synthesis of an arylboronic acid-based solid-phase amidation catalyst. *Synthesis* **2001**, 1611–1613.

(31) Yang, W.; Gao, X.; Springsteen, G.; Wang, B. Catechol pendant polystyrene for solid-phase synthesis. *Tetrahedron Lett.* **2002**, 6339–6342.

(32) Di Costanzo, L.; Sabio, G.; Mora, A.; Rodriguez, P. C.; Ochoa, A. C.; Centeno, F.; Christianson, D. W. Crystal structure of human arginase I at 1.29-angstrom resolution and exploration of inhibition in the immune response. *Proc. Natl. Acad. Sci. U.S.A.* **2005**, *102*, 13058–13063.

(33) Benini, S.; Rypniewski, W. R.; Wilson, K. S.; Mangani, S.; Ciurli, S. Molecular details of urease inhibition by boric acid: insights into the catalytic mechanism. *J. Am. Chem. Soc.* **2004**, *126*, 3714–3715.

(34) Chen, Y.; Shoichet, B.; Bonnet, R. Structure, function, and inhibition along the reaction coordinate of CTX-M beta-lactamases. *J. Am. Chem. Soc.* **2005**, *127*, 5423–5434.

(35) Stolowitz, M. L.; Ahlem, C.; Hughes, K. A.; Kaiser, R. J.; Kesicki, E. A.; Li, G.; Lund, K. P.; Torkelson, S. M.; Wiley, J. P. Phenylboronic acid−salicylhydroxamic acid bioconjugates. 1. A novel boronic acid complex for protein immobilization. *Bioconjugate Chem.* **2001**, *12*, 229–239.

(36) Paugam, M.-F.; Bien, J. T.; Smith, B. D.; Chrisstoffels, L. A. J.; deJong, F.; Reinhoudt, D. N. Facilitated catecholamine transport through bulk and polymer-supported liquid membranes. *J. Am. Chem. Soc.* **1996**, *118*, 9820–9825.

(37) Duggan, P. J. Fructose-permeable liquid membranes containing boronic acid carriers. *Aust. J. Chem.* **2004**, *57*, 291–299.

(38) Smith, B. D. In *Advances in Supramolecular Chemistry*; Gokel, G. W., Ed.; JAI Press: Greenwich, CT, 1999; vol. 5, pp 157−202.

(39) Westmark, P. R.; Gardiner, S. J.; Smith, B. D. Selective monosaccharide transport through lipid bilayers using boronic acid carriers. *J. Am. Chem. Soc.* **1996**, *118*, 11093–11100.

(40) Chen, Y.; Bastow, K. F.; Goz, B.; Kucera, L.; Morris-Natschke, S. L.; Ishaq, K. S. Boronic acid derivatives targeting HIV-1. *Antiviral Chem. Chemother.* **1996**, *7*, 108–114.

(41) Miller, J. F.; Andrews, C. W.; Brieger, M.; Furfine, E. S.; Hale, M. R.; Hanlon, M. H.; Hazen, R. J.; Kaldor, I.; McLean, E. W.; Reynolds, D.; Sammond, D. M.; Spaltenstein, A.; Tung, R.; Turner, E. M.; Xu, R. X.; Sherrill, R. G. Ultra-potent P1 modified arylsulfonamide HIV protease inhibitors: the discovery of GW0385. *Bioorg. Med. Chem. Lett.* **2006**, *16*, 1788–1794.

(42) Frantzen, F.; Grimsrud, K.; Heggli, D. E.; Sundrehagen, E. Soluble highly coloured phenylboronic acids and their use in glycohemoglobin quantification. *Clin. Chim. Acta* **1997**, *263*, 207–224.

(43) Shull, B. K.; Spielvogel, D. E.; Gopalaswamy, R.; Sankar, S.; Boyle, P. D.; Head, G.; Devito, K. Evidence for spontaneous, reversible paracyclophane formation. Aprotic solvation structure of the boron neutron capture therapy drug, L-*p*-boronophenylaline. *J. Chem. Soc., Perkin Trans.* **2000**, *2*, 557–561.

(44) Srivastava, R. R.; Singhaus, R. R.; Kabalka, G. W. 4-Dihydroxyborylphenyl analogues of 1-aminocyclobutanecarboxylic acids: potential boron neutron capture therapy agents. *J. Org. Chem.* **1999**, *64*, 8495–8500.

(45) Barth, R. F.; Grecula, J. C.; Yang, W.; Rotaru, B. J.; Ferketich, A. K.; Moeschberger, M. L.; Coderra, J. A.; Rofstad, E. K. Combination of boron neutron capture therpy and external beam radiotherapy for brain tumors. *Int. J. Radiat. Oncol. Biol. Phys.* **2004**, *58*, 267–277.

(46) Adams, J.; Behnke, M.; Chen, S.; Cruickshank, A. A.; Dick, L. R.; Grenier, L.; Klunder, J. M.; Ma, Y. T.; Plamondon, L.; Stein, R. L. Potent and selective inhibitors of the proteasome: dipeptidyl boronic acids. *Bioorg. Med. Chem. Lett.* **1998**, *8*, 333–338.

(47) Adams, J.; Kaufmann, M. Development of the proteasome inhibitor velcade (bortezomib). *Cancer Invest.* **2004**, *22*, 304–311.

(48) Fahy, B. N.; Schlieman, M. G.; Virudachalam, S.; Bold, R. J. Schedule-dependent molecular effects of the proteasome inhibitor bortezomib and gemcitabine in pancreatic cancer. *J. Surg. Res.* **2003**, *113*, 88–95.

(49) Nawrocki, S. T.; Carew, J. S.; Pino, M. S.; Highshaw, R. A.; Andtbacka, R. H. I.; Dunner, K.; Pal, A.; Bornmann, W. G.; Chiao, P. J.; Huang, P.; Xiong, H.; Abbruzzese, J. L.; McConkey, D. J. Aggresome disruption: a novel strategy to enhance bortezomib-induced apoptosis in pancreatic cancer cells. *Cancer Res.* **2006**, *66*, 3773–3781.

(50) Nawrocki, S. T.; Carew, J. S.; Pino, M. S.; Highshaw, R. A.; Dunner, K.; Huang, P.; Abbruzzese, J. L.; McConkey, D. J. Bortezomib sensitizes pancreatic cancer cells to endoplasmic reticulum stress-mediated apoptosis. *Cancer Res.* **2005**, *65*, 11658–11666.

(51) McCormack, T.; Baumeister, W.; Grenier, L.; Moomaw, C.; Plamondon, L.; Pramanik, B.; Slaughter, C.; Soucy, F.; Stein, R. L.; Zuhl, G.; Dick, L. R. Active site-directed inhibitors of phodococcus 20 S proteasome: kinetics and mechanism. *J. Biol. Chem.* **1997**, *272*, 26103–26109.

(52) Pekol, T.; Daniels, J. S.; Labutti, J.; Parsons, I.; Nix, D.; Baronas, E.; Hsieh, F.; Gan, L.-S.; Miwa, G. Human metabolism of the proteasome inhibitor bortezomib: identification of circulating metabolites. *Drug Metab. Dispos.* **2005**, *33*, 771–777.

(53) Labutti, J.; Pearsons, I.; Huang, R.; Miwa, G.; Gan, L.-S.; Daniels, J. S. Oxidative deboronation of the peptide boronic acid proteosome inhibitor bortezomib: contributions from reactive oxygen species in this novel cytochrome P450 reaction. *Chem. Res. Toxicol.* **2006**, *19*, 539–546.

(54) Lindquist, R. N.; Nguyen, A. C. Aminomethaneboronic acids. Synthesis and inhibition of boron analogue of esterase substrates. *J. Am. Chem. Soc.* **1977**, *99*, 6435–6437.

(55) Dembitsky, V. M.; Quntar, A. A.; Srebnik, M. Recent advances in the medicinal chemistry of alpha-aminoboronic acids, amine−carboxyboranes and their derivatives. *Mini Rev. Med. Chem.* **2004**, *4*, 1001–1018.

(56) Amssoms, B. K.; Oza, S. L.; Ravaschino, E.; Yamani, A.; Lambeir, A.; Rajan, P.; Bal, G.; Rodriguez, J.; Fairlamb, A. H.; Augustyns, K.; Haemers, A. Glutathione-like tripeptides as inhibitors of glutathionylspermidine synthetase. Part 1: Substitution of the glycine carboxylic acid group. *Bioorg. Med. Chem. Lett.* **2002**, *12*, 2553–2556.

(57) Møller, C.; Pesset, M. S. Note on an approximation treatment for many-electron systems. *Pure Appl. Chem.* **1934**, *46*, 618–622.

(58) Dunning, T. H., Jr. Gaussian basis sets for use in correlated molecular calculations. I. The atoms boron through neon and hydrogen. *J. Chem. Phys.* **1989**, *90*, 1007–1023.

(59) Woon, D. E.; Dunning, T. H., Jr. Gaussian basis sets for use in correlated molecular calculations. III. The atoms aluminum through argon. *J. Chem. Phys.* **1993**, *98*, 1358–1371.

(60) Kendall, R. A.; Dunning, T. H., Jr.; Harrison, R. J. Electron affinities of the first-row atoms revisited. Systematic basis sets and wave functions. *J. Chem. Phys.* **1992**, *96*, 6796–6806.

(61) Peterson, K. A.; Woon, D. E.; Dunning, T. H., Jr. Benchmark calculations with correlated molecular wave functions. IV. The classical barrier height of the $H + H_2 \rightarrow H_2 + H$ reaction. *J. Chem. Phys.* **1994**, *100*, 7410–7415.

(62) Gonzalez, C.; Schlegel, H. B. An improved algorithm for reaction path following. *J. Chem. Phys.* **1989**, *90*, 2154–2161.

(63) Gonzalez, C.; Schlegel, H. B. Reaction path following in mass-weighted internal coordinates. *J. Phys. Chem.* **1990**, *94*, 5523–5527.

(64) Frisch, M. J.; Trucks, G. W.; Schlegel, H. B.; Scuseria, G. E.; Robb, M. A.; Cheeseman, J. R.; Montgomery, J. A., Jr.; Vreven, T.; Kudin, K. N.; Burant, J. C.; Millam, J. M.; Iyengar, S. S.; Tomasi, J.; Barone, V.; Mennucci, B.; Cossi, M.; Scalmani, G.; Rega, N.; Petersson, G. A.; Nakatsuji, H.; Hada, M.; Ehara, M.; Toyota, K.; Fukuda, R.; Hasegawa, J.; Ishida, M.; Naskajima, T.; Honda, Y.; Kitao, O.; Nakai, H.; Klene, M.; Li, X.; Knox, J. E.; Hratchian, H. P.; Cross, J. B.; Adamo, C.; Jaramillo, J.; Gomperts, R.; Stratmann, R. E.; Yazyev, O.; Austin, A. J.; Cammi, R.; Pomelli, C.; Ochterski, J. W.; Ayala, P. Y.; Morokuma, K.; Voth, G. A.; Salvador, P.; Dannenberg, J. J.; Zakrzewski, V. G.; Dapprich, S.; Daniels, A. D.; Strain, M. C.; Farkas, O.; Malick, D. K.; Rabuck, A. D.; Raghavachari, K.; Foresman, J. B.; Ortiz, J. V.; Cui, Q.; Baboul, A. G.; Clifford, S.; Cioslowski, J.; Stefanov, B. B.; Liu, G.; Liashenko, A.; Piskorz, P.; Komaromi, I.; Martin, R. L.; Fox, D. J.; Keith, T.; Al-Laham, M. A.; Peng, C. Y.; Nanayakkara, A.; Challacombe, M.; Gill, P. M. G.; Johnson, B.; Chen, W.; Wong, M. W.; Gonzalez, C.; Pople, J. A. *Gaussian 03*, revision B.02; Gaussian, Inc.: Wallingford, CT, 2003.

(65) Carpenter, J. E.; Weinhold, F. Analysis of the geometry of the hydroxymethyl radical by the "different hybrids for different spins" natural bond orbital procedure. *THEOCHEM* **1988**, *169*, 41–62.

(66) Curtiss, L. A.; Weinhold, F. Intermolecular interactions from a natural bond orbital. *Chem. Rev.* **1988**, *88*, 899–926.

(67) Foster, J. P.; Weinhold, F. Natural hybrid orbitals. *J. Am. Chem. Soc.* **1980**, *102*, 7211–7218.

(68) Reed, A. E.; Weinstock, R. B.; Weinhold, F. Natural population analysis. *J. Chem. Phys.* **1985**, *83*, 735–746.

(69) Clark, T.; Chandrasekhar, J.; Spitznagel, G. W.; Von Ragué Schleyer, P. Efficient diffuse function-augmented basis sets for anion calculations. III. The 3-21+G basis set for first-row elements, Li−F. *J. Comput. Chem.* **2004**, *4*, 294–301.

(70) Krishnan, R.; Binkley, J. S.; Seeger, R.; Pople, J. A. Self-consistent molecular orbital methods. XX. A basis set for correlated wave functions. *J. Chem. Phys.* **1980**, *72*, 650–654.

(71) Feng Xue, Q. L.; Mak, T. C. W. Crystalline inclusion compounds of urea with oxoboron compounds. Stabilization of the elusive dihydrogen borate anion in a hydrogen-bonded host lattice. *Inorg. Chem.* **1999**, *38*, 4142–4135.

(72) Perdew, J. P.; Burke, K.; Ernzerhof, M. Errata: Generalized gradient approximation made simple. *Phys. Rev. Lett.* **1997**, *78*, 1396.

(73) Bhat, K. L.; Braz, V.; Laverty, E.; Bock, C. W. The effectiveness of a primary aliphatic amino group as an internal Lewis base on the formation of a boron-oxygen-carbon linkage: a computational study. *THEOCHEM* **2004**, *712*, 9–19.

(74) Bhat, K. L.; Hakik, S.; Carvo, J. N.; Marycz, D. M.; Bock, C. W. A computational study of the formation of 1,3,2-dioxaborolane from the reaction of dihydroxy borane with 1,2-ethanediol. *THEOCHEM* **2004**, *673*, 145–154.

(75) Bhat, K. L.; Howard, N. J.; Rostami, H.; Lai, J. H.; Bock, C. W. Intramolecular dative bonds involving boron with oxygen and nitrogen in boronic acids and esters: a computational study. *THEOCHEM* **2005**, *723*, 147–157.

(76) Larkin, J. D.; Bhat, K. L.; Markham, G. D.; Brooks, B. R.; Lai, J. H.; Bock, C. W. A computational investigation of the geometrical structure and protodeboronation of Boroglycine. *J. Phys. Chem. A* **2007**, *111*, 6489–6500.

(77) Larkin, J. D.; Bhat, K. L.; Markham, G. D.; Brooks, B. R.; Schaefer, H. F., III.; Bock, C. W. Structure of the boronic acid dimer and the relative stabilities of its conformers. *J. Phys. Chem. A* **2006**, *110*, 10633–10642.

(78) Larkin, J. D.; Milkevitch, M.; Bhat, K. L.; Markham, G. D.; Brooks, B. R.; Bock, C. W. Dimers of boroglycine and methylamine boronic acid: a computational comparison of the relative importance of dative versus hydrogen bonding. *J. Phys. Chem. A.* **2008**, *112*, 125–133.

(79) Le Tourneau, H. A.; Birsch, R. E.; Korbeck, G.; Radkiewicz-Poutsma, J. L. Study of the dative bond in 2-amino ethoxydiphenyl borate at various levels of theory: another poor performance of the B3LYP method for B−N dative bonds. *J. Phys. Chem. A* **2005**, *109*, 12014–12019.

(80) Gilbert, T. M. Tests of the MP2 model and various DFT models in predicting the structures and B−N bond dissociation energies of amine−boranes $(X_3C)_mH_{3-m}B-N(CH_3)_nH_3$: poor performance of the B3LYP approach for dative B−N bonds. *J. Phys. Chem. A* **2004**, *108*, 2550–2554.

(81) Cances, E.; Mennucci, B.; Tomasi, J. A new integral equation formalism for the polarizable continuum model: theoretical background and applications to isotropic and anisotropic dielectrics. *J. Chem. Phys.* **1997**, *1007*, 3032–3041.

(82) Cossi, M.; Barone, V.; Mennucci, B.; Tomasi, J. Ab initio study of ionic solutions by a polarizable continuum dielectric model. *Chem. Phys. Lett.* **1998**, *286*, 253–260.

(83) Cossi, M.; Scalmani, G.; Rega, N.; Barone, V. New developments in the polarizable continuum model for quantum mechanical and classical calculations on molecules in solution. *J. Chem. Phys.* **2002**, *117*, 43–54.

(84) Mennucci, B.; Cances, E.; Tomasi, J. Evaluation of solvent effects in isotropic and anisotropic dielectrics and in ionic solutions with a unified integral equation method: theoretical bases, computational implementation, and numerical applications. *J. Phys. Chem. B* **1997**, *101*, 10506–10517.

(85) Mennucci, B.; Tomasi, J. Continuum solvation models: a new approach to the problem of solute's charge distribution and cavity boundaries. *J. Chem. Phys.* **1997**, *106*, 5151–5158.

(86) We wish to note that we previously reported (*J. Phys. Chem. A* **2008**, *112*, 125−133.) COSMO-RS values that were indeed computed using only COSMO methodology.

(87) Barone, V.; Cossi, M. Quantum calculation of molecular energies and energy gradients in solution by a conductor solvent model. *J. Phys. Chem. A* **1998**, *102*, 1995–2001.

(88) Cossi, M.; Scalmani, G.; Rega, N.; Barone, V. Energies, structures, and electronic properties of molecules in solution with the C-PCM solvation model. *J. Comput. Chem.* **2003**, *24*, 669–681.

(89) Takano, Y.; Houk, K. N. Benchmarking the conductor-like polarizable continuum model (CPCM) for aqueous solvation free energies of neutral and ionic organic molecules. *J. Chem. Theory Comput.* **2005**, *1*, 70–77.

(90) Castejon, H.; Wiberg, K. B. Solvent effects on methyl transfer reactions. 1. The Menshutkin reaction. *J. Am. Chem. Soc.* **1999**, *121*, 2139–2146.

(91) Castejon, H.; Wiberg, K. B.; Sklenak, S.; Hinz, W. Solvent effects on methyl transfer reactions. 2. The reaction of amines with trimethylsulfonium salts. *J. Am. Chem. Soc.* **2001**, *123*, 6092–6097.

(92) Matteson, D. S. *Stereodirected Synthesis with Organoboranes*; Springer: Berlin, 1995.

(93) In the absence of experimental data for reaction 1, it seemed wise to establish the reliability of our calculations as best we could. The enthalpy for the hydrolysis reaction of methylboronic acid ($H_3C-B(OH)_2$), $H_3CB(OH)_2 + H_2O\ CH_4 + B(OH)_3$, has been reported to be −26.8 kcal/mol on the basis of published heat-of-formation data (298 K) for the molecules in this reaction.[97] The calculated values of ΔH for this hydrolysis in vacuo were −27.9, −27.8, −21.5, and −30.5 kcal/mol at the PBE1PBE/6-311++G(d,p), MP2/cc-pVDZ, MP2/aug-cc-pVDZ, and MP2/cc-pVTZ, respectively. It is of interest to note that the calculated values of ΔH for the analogous hydrolysis reaction of boroglycine, $H_2N-CH_2-B(OH)_2 + H_2O\ H_2N-CH_3 + B(OH)_3$, were −29.2, −31.9, −26.1, −30.8, and −30.3 kcal/mol. Therefore, the presence of a basic primary amine group in the R-position appears to play a relatively minor role in the thermodynamics of this hydrolysis.

(94) Matteson, D. S.; Sadhu, K. M. Synthesis of 1-amino-2-phenylethane-1-boronic acid derivatives. *Organometallics* **1984**, *3*, 614–618.

(95) Laplante, C.; Hall, D. G. Direct mono-*N*-methylation of solid-supported amino acids: a useful application of the Matteson rearrangement of alpha-aminoalkylboronic esters. *Org. Lett.* **2001**, *3*, 1487–1490.

(96) Amiri, P.; Lindquist, R. N.; Matteson, D. S.; Sadhu, K. M. Benzamidomethaneboronic acid: synthesis and inhibition of chymotrypsin. *Arch. Biochem. Biophys.* **1984**, *234*, 531–536.

(97) Duncan, K.; Faraci, W. S.; Matteson, D. S.; Walsh, C. T. (1-Aminoethyl)boronic acid: a novel inhibitor for *Bacillus stearothermophilus* alanine racemase and *Salmonella typhimurium*D-alanine:D-alanine ligase (ADP-forming). *Biochemistry* **1989**, *28*, 3541–3549.

(98) Dembitsky, V. M.; Srebnik, M. Synthesis and biological activity of alpha-aminoboronic acids, amine-carboxyboranes, and their derivatives. *Tetrahedron* **2003**, *59*, 579–593.

(99) Budzelaar, P. H. M.; Blok, A. N. J. Mechanism of oxidation of (olefin)RH1 and−Ir1 complexes by H_2O_2. *Eur. J. Inorg. Chem.* **2004**, 2385–2391.

(100) Kuivila, H. G. Electrophilic displacement reactions. III. Kinetics of the reaction between hydrogen peroxide and benzeneboronic acid. *J. Am. Chem. Soc.* **1954**, *76*, 870–874.

(101) Kuivila, H. G.; Armour, A. G. Electronic displacement reactions. IX. Effects of substituents on rates of reactions between hydrogen peroxide and benzeneboronic acid. *J. Am. Chem. Soc.* **1957**, *79*, 5659–5662.

(102) Paugam, M.-F.; Bien, J. T.; Smith, B. D.; Chrisstoffels, L. A. J.; de Jong, F.; Reinhoudt, D. N. Facilitated catecholamine transport through bulk and polymer-supported liquid membranes. *J. Am. Chem. Soc.* **1996**, *118*, 9820–9825.

JP904149W